



Doping concentration dependence of the photoluminescence spectra of n-type GaAs nanowires

Shermin Arab, Maoqing Yao, Chongwu Zhou, P. Daniel Dapkus, and Stephen B. Cronin

Citation: [Applied Physics Letters](#) **108**, 182106 (2016); doi: 10.1063/1.4947504

View online: <http://dx.doi.org/10.1063/1.4947504>

View Table of Contents: <http://scitation.aip.org/content/aip/journal/apl/108/18?ver=pdfcov>

Published by the [AIP Publishing](#)

Articles you may be interested in

[Self-catalyzed Ga\(N\)AsP nanowires and GaAsP/GaNAsP core-shell nanowires grown on Si \(111\) by gas-source molecular beam epitaxy](#)

J. Vac. Sci. Technol. B **34**, 02L108 (2016); 10.1116/1.4941133

[Electrical characterization and transport model of n-gallium nitride nanowires](#)

Appl. Phys. Lett. **107**, 082103 (2015); 10.1063/1.4929439

[Surface passivation of tellurium-doped GaAs nanowires by GaP: Effect on electrical conduction](#)

J. Appl. Phys. **115**, 234305 (2014); 10.1063/1.4883960

[GaAs nanowires grown on Al-doped ZnO buffer layer](#)

J. Appl. Phys. **114**, 084309 (2013); 10.1063/1.4819797

[Effect of Si-doping on InAs nanowire transport and morphology](#)

J. Appl. Phys. **110**, 053709 (2011); 10.1063/1.3631026

The image shows the cover of the journal Applied Physics Reviews. It features a blue and orange color scheme with a molecular structure background. The text 'NEW Special Topic Sections' is prominently displayed in white. Below it, 'NOW ONLINE' is written in orange, followed by 'Lithium Niobate Properties and Applications: Reviews of Emerging Trends' in white. The AIP Applied Physics Reviews logo is in the bottom right corner.

NEW Special Topic Sections

NOW ONLINE
Lithium Niobate Properties and Applications:
Reviews of Emerging Trends

AIP Applied Physics Reviews

Doping concentration dependence of the photoluminescence spectra of *n*-type GaAs nanowires

Shermin Arab,^{1,2} Maoqing Yao,^{1,2} Chongwu Zhou,^{1,2,3} P. Daniel Dapkus,^{1,2,3,4} and Stephen B. Cronin^{1,2,3,a)}

¹Department of Electrical Engineering, University of Southern California, Los Angeles, California 90089-0271, USA

²Center for Energy Nanoscience, University of Southern California, Los Angeles, California 90089-0271, USA

³Department of Chemical Engineering and Materials Science, University of Southern California, Los Angeles, California 90089-0271, USA

⁴Department of Physics, University of Southern California, Los Angeles, California 90089-0271, USA

(Received 6 September 2015; accepted 13 April 2016; published online 6 May 2016)

In this letter, the photoluminescence spectra of *n*-type doped GaAs nanowires, grown by the metal organic chemical vapor deposition method, are measured at 4 K and 77 K. Our measurements indicate that an increase in carrier concentration leads to an increase in the complexity of the doping mechanism, which we attribute to the formation of different recombination centers. At high carrier concentrations, we observe a blueshift of the effective band gap energies by up to 25 meV due to the Burstein-Moss shift. Based on the full width at half maximum (FWHM) of the photoluminescence peaks, we estimate the carrier concentrations for these nanowires, which varies from $6 \times 10^{17} \text{ cm}^{-3}$ (lightly doped), to $1.5 \times 10^{18} \text{ cm}^{-3}$ (moderately doped), to $3.5 \times 10^{18} \text{ cm}^{-3}$ (heavily doped) as the partial pressure of the disilane is varied from 0.01 sccm to 1 sccm during the growth process. We find that the growth temperature variation does not affect the radiative recombination mechanism; however, it does lead to a slight enhancement in the optical emission intensities. For GaAs nanowire arrays measured at room temperature, we observe the same general dependence of band gap, FWHM, and carrier concentration on doping. *Published by AIP Publishing.* [<http://dx.doi.org/10.1063/1.4947504>]

GaAs nanowires' direct band gap and large surface-to-volume ratio have attracted considerable attention for their potential use in high efficiency solar cells, energy storage, and lasers.^{1–5} Measuring the concentrations of the dopants in III-V nanowires and specifically GaAs nanowires is an important problem since it governs the mobility, minority carrier diffusion length/lifetime, and conductivity. This fact becomes even more important when one designs PN, PIN, or core-shell nanowires where concentrations of dopants and doping profiles directly affect the performance of the junction. While accurate measurement of carrier concentration in GaAs nanowires is of great importance, precise measurement techniques of these carrier concentrations have not been developed yet. In previous literature, both contact and non-contact methods have been employed for estimating carrier concentrations in III-V nanowires. Field effect measurements are one way of obtaining the field effect mobility and carrier concentration.⁶ However, this method presents several limitations and technical challenges, for example, formation of Ohmic contacts. Atom probe microscopy and secondary ion mass spectroscopy are two alternative methods used for establishing the doping profiles in nanowires; however, they are time consuming, expensive, and destructive to the sample being measured.⁷ Capacitance-voltage measurements present another approach that is commonly used,^{8,9} although this method also suffers from contact fabrication difficulties. Storm *et al.* reported Hall effect

measurements on core-shell InP nanowires.¹⁰ Schaper *et al.* also used Hall measurements with four contacts to obtain the carrier concentrations in InAs nanowires, as well as the electron concentrations in the surface accumulation layer of their InAs nanowires.¹¹ It should be noted that the Hall method has not been implemented in GaAs nanowires due to difficulties in forming Ohmic contacts. Ketterer *et al.* reported a non-contact method that correlates the carrier concentration of *p*-type GaAs nanowires with transmission Raman spectroscopy.¹² This method is based on forward Raman scattering, and it is unlikely that nanowires with large diameters (larger than 250 nm) will provide enough signal intensity for this measurement approach to be feasible. It should be noted that Raman scattering measurements have been reported from UHV-cleaved bulk GaAs (110) orientation. However, this case is valid only when samples are excited by light source with energy equal or larger than the band gap.¹³ Chen *et al.* studied the temperature effects on the photoluminescence (PL) spectra of bulk metal organic vapor phase epitaxy (MOVPE) grown GaAs films.¹⁴ The photoluminescence (PL) spectra of molecular beam epitaxy (MBE) grown bulk GaAs was studied at 4.2 K, as reported in Ref. 15. Both *n*-type doped¹⁶ and *p*-type doped GaAs^{17,18} were studied. Lee *et al.* performed a room temperature PL analysis and proposed a model where the PL peak energy can be estimated from the carrier concentrations.¹⁶ Kim *et al.* performed a similar analysis for C-doped samples at 12 K and proposed imperial relations for hole concentration estimations based on the FWHM of the PL peaks.¹⁷ Optical pump terahertz probe spectroscopy has been used to estimate the doping

^{a)}Author to whom correspondence should be addressed. Electronic mail: scronin@usc.edu.

density and carrier mobility at room temperature for Vapor liquid solid (VLS) grown nanowires.^{19–22} Wang *et al.* spatially resolved doping concentration and non-radiative recombination rate by using micro-photoluminescence which allows room temperature measurement without ultra-high vacuum.²³ Lindgren *et al.* compared the carrier concentration obtained from photoluminescence and Hall measurement and found excellent agreement.²⁴ Most of the studies focused on VLS or MBE grown nanowires and less attention has been paid to the doping study of nanowires synthesized by selective area MOCVD growth, in spite of its potential in large scale production of functional devices.^{25,26} The growth mechanism and thus principles of dopant incorporate differ to a large extent among different growth techniques due to variations in surface chemistry, precursor decomposition, and adatom migration. Non-uniform doping²⁷ and reservoir effect²⁸ have been observed for VLS grown nanowires and polytypism often occurs or is manipulated, which also alter the optical properties of VLS grown nanowires.²⁹ On the other hand, in selective area MOCVD, the growth is governed by vapor phase deposition instead of the thermal dynamics at the triple-phase interface in VLS. For all the samples studied, we do not observe any Wurtzite phase although there is a high density of rotational twins with an average spacing of 20 nm between adjacent twins. Shimamura *et al.* showed that carrier scattering due to twin is minimal if their spacing is larger than 5 nm.³⁰ Here, we present a systematic study of the carrier concentration of *n*-type doped GaAs nanowires grown by selective area MOCVD using low-temperature and room temperature photoluminescence spectroscopy. The advantage of this method is that it is contact-less and does not require complex lithographic processing.

In this work, nanowires are grown on Si(111) substrate using MOCVD with selective area growth (SAG).³¹ These nanowires are grown vertically along the (111)B direction, as shown in Figure 1(a), sonicated in isopropyl alcohol, and then deposited onto Si substrates with 300 nm of SiO₂ (Figure 1(b)). Photoluminescence spectroscopy is collected using a 532 nm continuous-wave laser.³²

Figure 1 shows SEM micrographs of a GaAs nanowire array and individual GaAs nanowires deposited on a Si/SiO₂ substrate. These nanowires are doped with Si, where Si behaves as a donor. Here, the diameters of the nanowires lie in the range of 250–270 nm. Radiative recombination in GaAs nanowires can arise from various mechanisms

including: direct band-band transition with momentum conservation, indirect band-band transition without momentum conservation, and indirect band-acceptor transition without momentum conservation.³³ The concentration of dopants governs which mechanism will be dominant in the radiative recombination process.

In Figure 2, PL spectra of the three cases of lightly, moderately, and heavily doped GaAs nanowires are shown. Since these PL spectra are complex, we attempt to assign the peaks to corresponding transitions. In Figure 2(a), two major peaks can be observed. The peak at 1.497 eV is due to the exciton,^{34–36} and the 1.449 eV peak is characteristic of a band-acceptor transition due to carbon contamination.³⁷ Wood *et al.* attributed the 1.454 eV peak to the phonon sideband of the band-to-acceptor transition at 1.490 eV.³⁷ Here, we observe the same phenomenon with a phonon energy of 36 meV. The peaks at 1.484 eV and 1.470 eV are also impurity related (free-to-bound transition).³⁸ In the lightly doped case, the blueshift is not observed, and the donor-band transition is not dominant. In Figure 2(b), three main peaks from the moderately Si-doped nanowires are observed. The peaks at 1.489 eV and 1.491 eV correspond to a band-acceptor transition due to unintentional carbon impurities. The peak at 1.533 eV indicates the donor-band transition and is blue-shifted by about 20 meV. Figure 2(c) shows the PL response of heavily Si-doped GaAs nanowires. Here, a blueshift of about 25 meV is observed (peak at 1.537 eV). The peak at 1.518 eV corresponds to an excitonic transition, as reported by Wood and Ploog.^{37,38} The peaks at 1.496, 1.488, 1.469, and 1.460 eV originate from acceptor impurity levels. It has been shown that, in the presence of high concentrations of Si dopants, the behavior of some dopant impurities may switch from donor to acceptor.^{39,40} The observed peaks between 1.480 and 1.490 eV are likely due to Si dopant impurities. Similar to the case of the lightly doped GaAs nanowires, the peak at approximately 1.450 eV is the phonon sideband of the 1.490 eV peak. The PL spectra of these samples were also measured at 77 K, as shown in Figure S1 of the supplementary material.⁴³ While the features in the 4 K spectra are a little sharper than those taken at 77 K, all of the same features can be resolved. Furthermore, the overall FWHM, which can be used to measure carrier concentration, are the same. This indicates that the spectra taken at 77 K are sufficient to resolve the features required to establish doping concentrations.

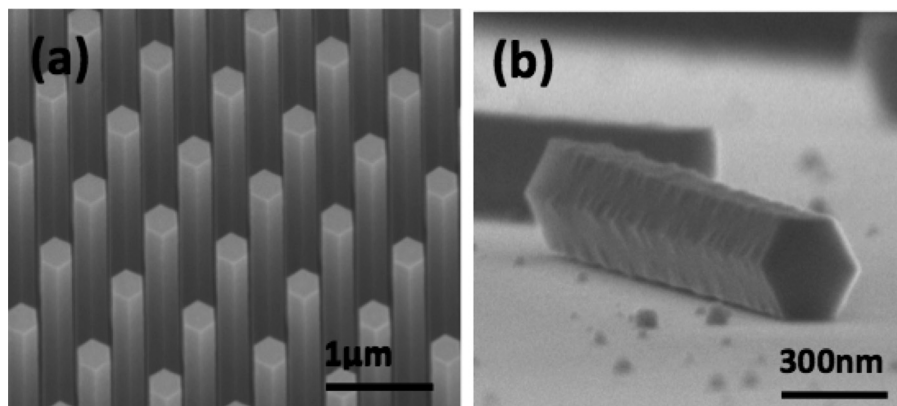


FIG. 1. SEM image of *n*-type doped GaAs (a) nanowire array and (b) individual nanowires on a Si/SiO₂ substrate.

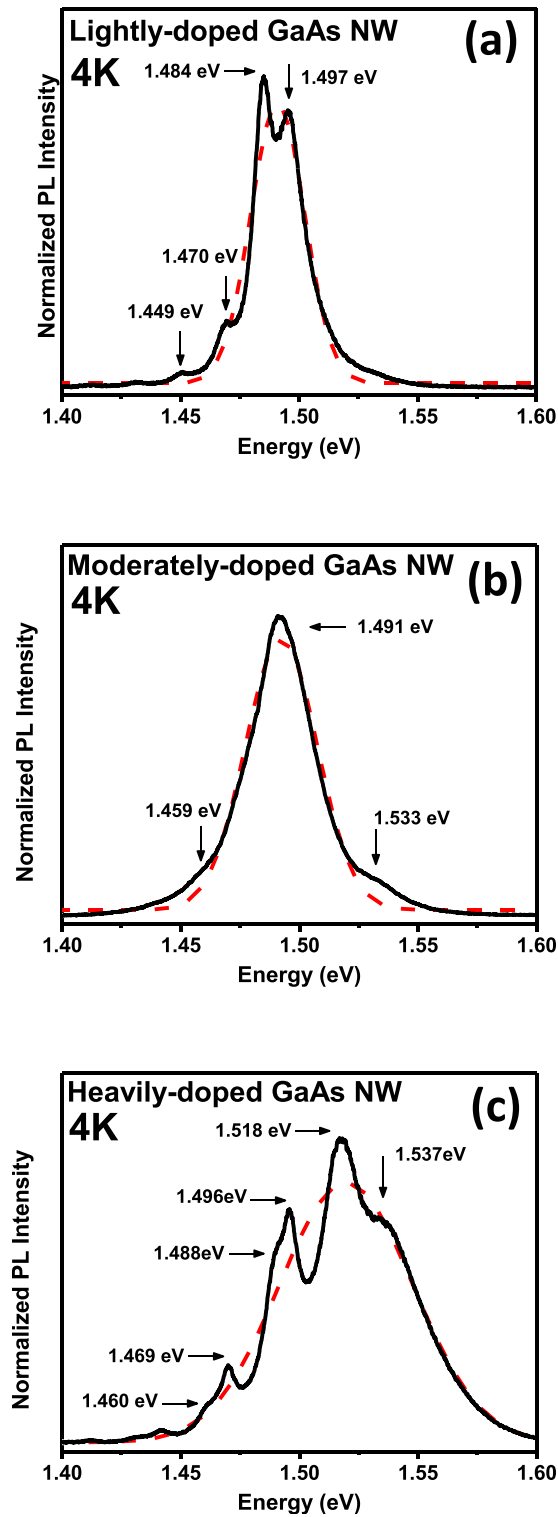


FIG. 2. Photoluminescence response of (a) lightly doped, (b) moderately doped, and (c) heavily doped *n*-type GaAs nanowires excited by a CW 532 nm laser at 4 K, the dashed line indicates the fitted curve for each case.

Based on previous literature for impurity levels below $5 \times 10^{17} \text{ cm}^{-3}$, the band-acceptor transition is dominant.³³ However, as the minority carrier concentration increases, the impurity level within the band gap (E_T) extends into the band, due to inhomogeneous dopant distributions and potential fluctuations (V_{rms}). The following formula is obtained for V_{rms} .⁴¹

$$V_{rms} = \left(\frac{e^2}{\epsilon} \right) [2\pi(N_D^+ + N_A^-)r_s]^{1/2},$$

where r_s is the screening length ($r_s = \left(\frac{a}{2}\right)(n \times a^3)^{-1/6}$) and a is the Bohr radius of the majority carriers; for moderate to heavily doped cases, we can assume $N_D^+ - N_A^- \sim n$. E_T can be calculated as

$$E_T = 2\pi^{1/2} \left(\frac{e^2}{\epsilon} \right) a^{1/4} n^{5/12}.$$

As the dopant concentration increases, E_T increases until it reaches the ionization energy ($E_A \sim 26.4 \text{ meV}$) of the C dopants and creates localized acceptor states.³³ An increase in n leads to the formation of a conducting impurity band in the energy gap and creation of free electrons. Therefore, the dominant transition would occur as an indirect band-acceptor transition between the free electrons in the conduction band and localized acceptor states in the impurity level within the band gap near the valance band (Figures 2(c) and S2 of the supplementary material⁴³).

In Figure 3(a), we use the empirical relation reported by De-Sheng *et al.* in order to estimate the carrier concentrations from the energy half-width (ΔE) of the dominant emission line in the PL spectra.³³

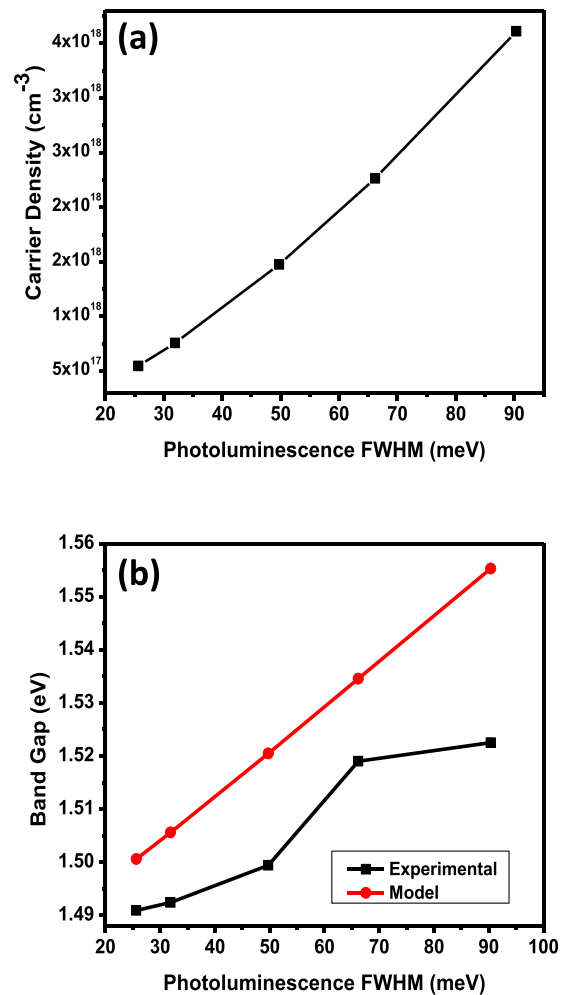


FIG. 3. (a) Carrier concentrations estimated from photoluminescence FWHM. (b) Effective band gap estimated from both experimental photoluminescence and model from reference.

$$\Delta E(n) = (3.84 \times 10^{-14})n^{2/3}.$$

Here, ΔE is measured in meV and n in cm^{-3} . We can also estimate the band gap variation as a function of dopant concentration using the indirect band-localized acceptor transition model, where E_g is given by

$$E_g = E_g^0 + E_F - E_T,$$

where E_g^0 is the band gap of non-doped GaAs and E_F can be derived from the work of Raymond *et al.*:⁴²

$$\begin{aligned} E_F &= \frac{\hbar^2}{2m_e^*} (3\pi^2 n)^{2/3} \left(1 - 0.8156 \frac{E_F}{E_g} \right) \\ &= 5.209 \times 10^{-14} (n^{2/3}) - 1.456 \times 10^{-27} (n^{4/3}). \end{aligned}$$

Using the above formula, we have calculated the expected bandgap from the photoluminescence FWHM and compared that to the experimental values. These results are plotted in Figure 3(b), where the experimental values and calculated values are in relatively close agreement. The experimental results show band gap values of approximately 10 meV below the calculated values, and the blueshift due to Pauli blocking in the band gap is evident. It should be noted that the model used for this calculation is valid for bulk material systems. Our measurements are on individual GaAs nanowire. Therefore, variation from the calculation is expected, considering the confinement and increased surface-to-volume ratio. We believe the general trend observed for the nanowires matches that of bulk, while the exact parameters in the model may deviate slightly.

We have performed room temperature measurements on arrays of GaAs nanowires grown on an underlying Si substrate over (111) surface. These nanowires are grown using the same recipe that was mentioned earlier and are doped using similar disilane flow rates (0 and 1 sccm in 0.1 sccm increments). The room temperature PL spectra obtained from these GaAs nanowire arrays are plotted in Figure 4. Here, the FWHM and the blueshift in the spectra are clearly observed at room temperature and can be used to estimate the carrier concentrations. An obvious increase in the band gap is observed from 1.4166 eV to 1.500 eV. The FWHM also increases, corresponding to carrier concentrations varying from 3×10^{17} to $2.2 \times 10^{18} \text{ cm}^{-3}$, as shown in Figure 4(b). For the room temperature data, the trend of photoluminescence blueshifting with increasing carrier concentration is observed as the disilane partial pressure is increased, and the range of estimated concentrations agrees with the 4 K measurements. However, for the most heavily doped case (1 sccm disilane flow), we observe a small drop in the FWHM and hence a decrease in carrier concentration. This is most likely due to the fact that Si is an amphoteric dopant in GaAs and can act as a donor or acceptor depending on whether or not it sits on a Ga or As site, respectively. At high doping concentrations, Si may behave as a *p*-type dopant leading to a decrease in the *n*-type carrier concentration and a corresponding redshift in the PL spectra.³⁹ This behavior is not observed our low temperature measurements due to coarse steps in variation of the disilane flow rate.

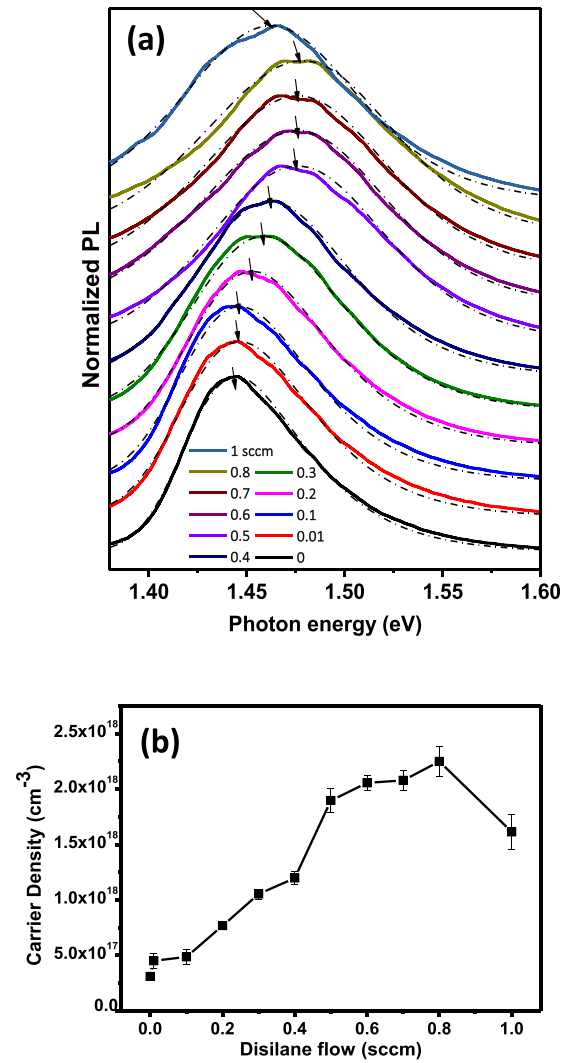


FIG. 4. (a) Room temperature photoluminescence spectra of doped GaAs nanowire arrays plotted for various disilane flow rates during the growth. (b) Estimated carrier concentrations plotted as a function of disilane flow rate.

In summary, we have estimated the carrier concentration in Si-doped MOCVD grown GaAs nanowires based on low temperature photoluminescence spectra using an indirect band-localized acceptor transition model. Using this model, we obtained concentrations of $6 \times 10^{17} \text{ cm}^{-3}$ (lightly doped), $1.5 \times 10^{18} \text{ cm}^{-3}$ (moderately doped), and $3.5 \times 10^{18} \text{ cm}^{-3}$ (heavily doped) for partial pressures of disilane varied from 0.01 sccm to 1 sccm during the growth process. At high carrier concentrations, we observe a blueshift in the effective band gap energy by up to 25 meV due to the Burstein-Moss shift (i.e., Pauli blocking). Our experimental band gap blueshift values are in agreement with the calculated blueshift values. The same general dependence of band gap, FWHM, and carrier concentration on doping is observed for GaAs nanowire arrays measured at room temperature. Although decrease in PL intensity (due to increase in non-radiative recombination) and PL spectral widening is observed at room temperature, the generality of carrier concentration estimates based on the photoluminescence FWHM is valid.

This material is based upon work supported as part of the Center for Energy Nanoscience (CEN), an Energy

Frontier Research Center (EFRC) funded by the U.S. Department of Energy, Office of Science and Office of Basic Energy Sciences, under Award No. DE-SC0001013.

- ¹J. Geisz, S. Kurtz, M. Wanlass, J. Ward, A. Duda, D. Friedman, J. Olson, W. McMahon, T. Moriarty, and J. Kiehl, "High-efficiency GaInP/GaAs/InGaAs triple-junction solar cells grown inverted with a metamorphic bottom junction," *Appl. Phys. Lett.* **91**(2), 023502 (2007).
- ²D. Saxena, S. Mokkapati, P. Parkinson, N. Jiang, Q. Gao, H. H. Tan, and C. Jagadish, "Optically pumped room-temperature GaAs nanowire lasers," *Nat. Photonics* **7**(12), 963–968 (2013).
- ³K. Tomioka, J. Motohisa, S. Hara, K. Hiruma, and T. Fukui, "GaAs/AlGaAs core multishell nanowire-based light-emitting diodes on Si," *Nano Lett.* **10**(5), 1639–1644 (2010).
- ⁴L. Yang, J. Motohisa, T. Fukui, L. X. Jia, L. Zhang, M. M. Geng, P. Chen, and Y. L. Liu, "Fabry-Pérot microcavity modes observed in the micro-photoluminescence spectra of the single nanowire with InGaAs/GaAs heterostructure," *Opt. Express* **17**(11), 9337–9346 (2009).
- ⁵D. Kang, S. Arab, S. B. Cronin, X. Li, J. A. Rogers, and J. Yoon, "Carbon-doped GaAs single junction solar microcells grown in multilayer epitaxial assemblies," *Appl. Phys. Lett.* **102**(25), 253902 (2013).
- ⁶C. Gutsche, I. Regolin, K. Blekker, A. Lysov, W. Prost, and F. J. Tegude, "Controllable p-type doping of GaAs nanowires during vapor-liquid-solid growth," *J. Appl. Phys.* **105**(2), 024305 (2009).
- ⁷D. E. Perea, E. R. Hemesath, E. J. Schwalbach, J. L. Lensch-Falk, P. W. Voorhees, and L. J. Lauhon, "Direct measurement of dopant distribution in an individual vapour-liquid-solid nanowire," *Nat. Nanotechnol.* **4**(5), 315–319 (2009).
- ⁸S. Roddaro, K. Nilsson, G. Astromskas, L. Samuelson, L.-E. Wernersson, O. Karlstrom, and A. Wacker, "InAs nanowire metal-oxide-semiconductor capacitors," *Appl. Phys. Lett.* **92**(25), 253509 (2008).
- ⁹R. Tu, L. Zhang, Y. Nishi, and H. Dai, "Measuring the capacitance of individual semiconductor nanowires for carrier mobility assessment," *Nano Lett.* **7**(6), 1561–1565 (2007).
- ¹⁰K. Storm, F. Halvardsson, M. Heurlin, D. Lindgren, A. Gustafsson, P. M. Wu, B. Monemar, and L. Samuelson, "Spatially resolved Hall effect measurement in a single semiconductor nanowire," *Nat. Nanotechnol.* **7**(11), 718–722 (2012).
- ¹¹C. Blömers, T. Grap, M. Lepsa, J. Moers, D. Grützmacher, H. Lüth, and T. Schäpers, "Hall effect measurements on InAs nanowires," *Appl. Phys. Lett.* **101**(15), 152106 (2012).
- ¹²B. Ketterer, E. Uccelli, and A. F. i Morral, "Mobility and carrier density in p-type GaAs nanowires measured by transmission Raman spectroscopy," *Nanoscale* **4**(5), 1789–1793 (2012).
- ¹³H. Stolz and G. Abstreiter, "Surface band bending on clean and oxidized (110)-GaAs studied by Raman spectroscopy," *Solid State Commun.* **36**(10), 857–860 (1980).
- ¹⁴Y. Chen, A. Freundlich, H. Kamada, and G. Neu, "Temperature effects on the photoluminescence of GaAs grown on Si," *Appl. Phys. Lett.* **54**(1), 45–47 (1989).
- ¹⁵P. Yu, D. Reynolds, and C. Stutz, "Sharp-line photoluminescence of GaAs grown by low-temperature molecular beam epitaxy," *Appl. Phys. Lett.* **61**(12), 1432–1434 (1992).
- ¹⁶N. Y. Lee, K. J. Lee, C. Lee, J. E. Kim, H. Y. Park, D. H. Kwak, H. C. Lee, and H. Lim, "Determination of conduction band tail and Fermi energy of heavily Si-doped GaAs by room-temperature photoluminescence," *J. Appl. Phys.* **78**(5), 3367–3370 (1995).
- ¹⁷S. I. Kim, M. S. Kim, Y. Kim, K. S. Eom, S. K. Min, and C. Lee, "Low temperature photoluminescence characteristics of carbon doped GaAs," *J. Appl. Phys.* **73**(9), 4703–4705 (1993).
- ¹⁸P. W. Yu and D. Reynolds, "Photoluminescence identification of ~77-meV deep acceptor in GaAs," *J. Appl. Phys.* **53**(2), 1263–1265 (1982).
- ¹⁹J. L. Boland, S. Conesa-Boj, P. Parkinson, G. Z. Tütüncüoglu, F. Matteini, D. Rüffer, A. Casadei, F. Amaduzzi, F. Jabeen, and C. L. Davies, "Modulation doping of GaAs/AlGaAs core-shell nanowires with effective defect passivation and high electron mobility," *Nano Lett.* **15**(2), 1336–1342 (2015).
- ²⁰H. J. Joyce, Q. Gao, H. H. Tan, C. Jagadish, Y. Kim, J. Zou, L. M. Smith, H. E. Jackson, J. M. Yarrison-Rice, and P. Parkinson, "III–V semiconductor nanowires for optoelectronic device applications," *Prog. Quantum Electron.* **35**(2), 23–75 (2011).
- ²¹P. Parkinson, H. J. Joyce, Q. Gao, H. H. Tan, X. Zhang, J. Zou, C. Jagadish, L. M. Herz, and M. B. Johnston, "Carrier lifetime and mobility enhancement in nearly defect-free core-shell nanowires measured using time-resolved terahertz spectroscopy," *Nano Lett.* **9**(9), 3349–3353 (2009).
- ²²S. Thunich, L. Prechtel, D. Spirkoska, G. Abstreiter, A. F. i Morral, and A. Holleitner, "Photocurrent and photoconductance properties of a GaAs nanowire," *Appl. Phys. Lett.* **95**(8), 083111 (2009).
- ²³F. Wang, Q. Gao, K. Peng, Z. Li, Z. Li, Y. Guo, L. Fu, L. M. Smith, H. H. Tan, and C. Jagadish, "Spatially resolved doping concentration and nonradiative lifetime profiles in single Si-doped InP nanowires using photoluminescence mapping," *Nano Lett.* **15**(5), 3017–3023 (2015).
- ²⁴D. Lindgren, O. Hultin, M. Heurlin, K. Storm, M. T. Borgström, L. Samuelson, and A. Gustafsson, "Study of carrier concentration in single InP nanowires by luminescence and Hall measurements," *Nanotechnology* **26**(4), 045705 (2015).
- ²⁵M. Yao, N. Huang, S. Cong, C.-Y. Chi, M. A. Seyedi, Y.-T. Lin, Y. Cao, M. L. Povinelli, P. D. Dapkus, and C. Zhou, "GaAs nanowire array solar cells with axial p–i–n junctions," *Nano Lett.* **14**(6), 3293–3303 (2014).
- ²⁶M. Yao, S. Cong, S. Arab, N. Huang, M. L. Povinelli, S. B. Cronin, P. D. Dapkus, and C. Zhou, "Tandem solar cells using GaAs nanowires on Si: Design, fabrication, and observation of voltage addition," *Nano Lett.* **15**(11), 7217–7224 (2015).
- ²⁷J. Dufouleur, C. Colombo, T. Garma, B. Ketterer, E. Uccelli, M. Nicotra, and A. Fontcuberta i Morral, "P-doping mechanisms in catalyst-free gallium arsenide nanowires," *Nano Lett.* **10**(5), 1734–1740 (2010).
- ²⁸K. A. Dick, J. Bolinsson, B. M. Borg, and J. Johansson, "Controlling the abruptness of axial heterojunctions in III–V nanowires: beyond the reservoir effect," *Nano Lett.* **12**(6), 3200–3206 (2012).
- ²⁹M. Heiss, S. Conesa-Boj, J. Ren, H.-H. Tseng, A. Gali, A. Rudolph, E. Uccelli, F. Peiró, J. R. Morante, and D. Schuh, "Direct correlation of crystal structure and optical properties in wurtzite/zinc-blende GaAs nanowire heterostructures," *Phys. Rev. B* **83**(4), 045303 (2011).
- ³⁰K. Shimamura, Z. Yuan, F. Shimojo, and A. Nakano, "Effects of twins on the electronic properties of GaAs," *Appl. Phys. Lett.* **103**(2), 022105 (2013).
- ³¹C.-C. Chang, C.-Y. Chi, M. Yao, N. Huang, C.-C. Chen, J. Theiss, A. W. Bushmaker, S. LaLumondiere, T.-W. Yeh, and M. L. Povinelli, "Electrical and optical characterization of surface passivation in GaAs nanowires," *Nano Lett.* **12**(9), 4484–4489 (2012).
- ³²S. Arab, P. D. Anderson, M. Yao, C. Zhou, P. D. Dapkus, M. L. Povinelli, and S. B. Cronin, "Enhanced Fabry-Pérot resonance in GaAs nanowires through local field enhancement and surface passivation," *Nano Res.* **7**(8), 1146–1153 (2014).
- ³³J. De-Sheng, Y. Makita, K. Ploog, and H. Queisser, "Electrical properties and photoluminescence of Te-doped GaAs grown by molecular beam epitaxy," *J. Appl. Phys.* **53**(2), 999–1006 (1982).
- ³⁴A. Cho and J. Arthur, "Molecular beam epitaxy," *Prog. Solid State Chem.* **10**, 157–191 (1975).
- ³⁵D. M. Collins, "The use of SnTe as the source of donor impurities in GaAs grown by molecular beam epitaxy," *Appl. Phys. Lett.* **35**(1), 67–70 (1979).
- ³⁶G. Stillman and C. Wolfe, "Electrical characterization of epitaxial layers," *Thin Solid Films* **31**(1), 69–88 (1976).
- ³⁷C. Wood and B. Joyce, "Tin-doping effects in GaAs films grown by molecular beam epitaxy," *J. Appl. Phys.* **49**(9), 4854–4861 (1978).
- ³⁸K. Ploog, A. Fischer, R. Trommer, and M. Hirose, "MBE-grown insulating oxide films on GaAs," *J. Vac. Sci. Technol.* **16**(2), 290–294 (1979).
- ³⁹J. Rossi, N. Holonyak, Jr., P. Dapkus, R. Burnham, and F. Williams, "Laser transitions in p-type GaAs: Si," *J. Appl. Phys.* **40**(8), 3289–3293 (1969).
- ⁴⁰J. Rossi, N. Holonyak, Jr., P. Dapkus, J. McNeely, and F. Williams, "Laser recombination transition in p-type GaAs," *Appl. Phys. Lett.* **15**(4), 109–110 (1969).
- ⁴¹H. Casey, Jr. and F. Stern, "Concentration-dependent absorption and spontaneous emission of heavily doped GaAs," *J. Appl. Phys.* **47**(2), 631–643 (1976).
- ⁴²A. Raymond, J. Robert, and C. Bernard, "The electron effective mass in heavily doped GaAs," *J. Phys. C: Solid State Phys.* **12**(12), 2289 (1979).
- ⁴³See supplementary material at <http://dx.doi.org/10.1063/1.4947504> for PL spectra of n-type doped GaAs nanowires measured at 77K.